Journal of Geology and Mining Research Vol. 4(6) pp. 118-129, November 2012
Available online http://www.academicjournals.org/jgmr
DOI: 10.5897/JGMR12.012
ISSN 2006 – 9766 ©2012 Academic Journals

Full Length Research Paper

Evaluating optimal well placement in horizontal drilling using geosteering: A case study of Agbada Field, Niger Delta

Ichenwo, John Lander and Dosunmu Adewale

Department of Petroleum Engineering, University of Port Harcourt, Rivers State, Nigeria.

Accepted 2 February, 2012

This study focuses on the use of geosteering technology in the optimal placement of wellbore path in Agbada 61 reservoir formation, where geological or subsurface target is far less than 100 m and where conventional approach could not be applicable. This was achieved by the formulation of a predrilled formation model from existing nearby or offset well by invertion of the resistivity log use in Agbada well 61, to get a squared Rt (true resistivity) profile (together with dip angles, to populate the aforementioned formation model). Then this tool response was calculated along the designed well path in stated formation model derived (that is, D7 sand). It was observed that exploitation of the D7 reservoir by using a slant well as advised by the operator would have placed the well path in the water zone but a horizontal well would exploit D7 reservoir sandstone optimally by placing the well path 10.7 ft away from the pseudo-water contact.

Key words: Geosteering, horizontal drilling, offset well, true resistivity.

INTRODUCTION

In conventional deviated drilling, the well path is steered according to a predetermined geometric plan defined by rigid boundaries and well plan and also drilled with conventional steering assemblies. The objective is to follow the line as closely as possible. Geosteering is a departure from this convention because it involves the use of logging while drilling (LWD) data to help place the horizontal wellbore in the proper position when the geological marker is ill defined, target tolerances are tight, or the geology is so complicated as to make conventional deviated drilling impractical (Al-Mutari et al., 2009).

One of the major problems when drilling horizontal wells in thin formations is to establish the well as horizontal in the objective formation. It is often the case that despite the best efforts of the well site personnel, the well becomes horizontal immediately above or below the target in the reservoir (Peach and Kloss, 1994). Geosteering enables the geological marker above the reservoir to be recognized and the final build to horizontal to be adjusted accordingly. Typically, gamma ray and resistivity tools are used to identify maker formations above the producing formation.

Geosteering refers to those activities designed to place the wellbore in a predetermined location, that location being defined by both its spatial coordinates, in three dimensions and by its position in the geological column. Proper geosteering will optimize wellbore placement in the productive reservoir, maximizing both drilling efficiency and hydrocarbon production. Early production, as well as the ultimate oil and gas recovery, from a reservoir often depends on the timeliness and the Geosteering decisions. Exiting the reservoir during drilling, results in costly and non-productive interval. Even remaining within the reservoir, but in a non-production location eventually leads to early water break through and leaves valuable oil behind. In recent years, the petroleum industry is looking for ways of detecting bed boundaries early so as to act on a timely fashion and also to know the direction of the conductive bed to prevent early exit from the reservoir (Omeragic et al., 2005).

Approaching the target is also a tough phase in the operation because the target's exact position is never really known as there are several geological uncertainties

*Corresponding author. E-mail: landerjohn2000@yahoo.com.

that mean the reservoir may be located higher or lower than expected. This may not be of enormous importance for a deviated or vertical well, but accuracy is crucial for a horizontal well.

STATEMENT OF PROBLEM

It was intended to drill a lateral well to a location west of the surface location in the D7.0 target sand. A pilot hole would be drilled to determine formation top and fluid contacts and then sidetracked to land in the lower D7.0 target. A Formation Junction was then set immediately at 72° inclination with 7" liner continuing from one leg of the junction to the D7.0 sand. The lateral would kick-off in 6" hole from the formation junction and 7" liner shoe.

Laterally, D7.0 was planned to land 26/27 ft TVD below the sand top and continues at 89.8° along an azimuth of 287° to a total depth close to the top of the sand. The drain hole was initially targeted at the lower lobe of the upper sand at the heel of the well, and then slowly transverses into the upper lobe. The planned length of the drain hole was 1500 ft.

A 12¼" pilot hole/main hole was drilled to a total depth of 9568 ftah (7471 ft SS) to locations close to the proposed landing targets. It was designed to serve as a build section for each of the laterals, thereby minimizing the amount of hole to be plugged back. After running pipe conveyed wireline logs the hole was under-reamed to 14¾" from the shoe to 7307 ftah and to 17½" from 7307 ftah down to 7415 ftah in preparation for running the FORM Junction.

Based on the pilot hole evaluation the drain hole position in the D4.0 sand was adjusted upwards by 16 ft TVD to 6774 ft SS. The D7.0 landing was not changed. At this point it was decided to sidetrack 12¼" hole and land the well in the D7.0 sand before running casing.

The pilot hole was plugged back and sidetracked from 8281 ftah at approximately 60° inclination using a 12¼" PDC bit and a 2.4° AKO setting on the motor. Once the sidetrack had been kicked-off, build rates of 5.4 to 8.9° were used to land the well. The well was landed 1 ft TVD higher then prognoses at 7314 ft SS (8857 ftah). The formation junction was set with the 7" liner shoe at 8857 ftah. The 7" liner shoe was drilled with a steerable assembly comprising of 4¾" Mach 1XL motor and 4¾" MPR tool. A 6" PDC bit was used in conjunction with a thruster at the top of the BHA to improve sliding. The drain hole was proposed to be slanted and drilled within a +/-3 ft TVD window of 7312 ft to 7318 ft SS but due to stalling mud motor and erratic tool face there was difficulty sliding hence the angle was inching up in rotary mode. The WOB was decreased to between 0-2 Klb and time drilled with the aim of dropping the angle but the angle kept on creeping up hence it was decided to stop drilling to avoid hitting the roof.

The XL motor and thruster provided good directional control in general, the only exception being deflections from the line when the mud motor was stalling while sliding and tool face that was erratic. The final total depth (TD) was 10162' MD, 91.85 and 291.0° Azi, 7310' SS and 3704' vertical section. Altogether a total length of 1305 feet of produceable sand was drilled through the pay zone from the casing shoe to TD at 10162 ftah.

The 4.5" liner was inadvertently dropped in hole while running in. All attempts to fish the liner were unsuccessful. A window was milled in the casing and an open-hole sidetrack was attempted. The well successfully kicked off from 8890 ft and an azimuthal turn was required to steer the well away from the fish. Final TD was 10359 ft MD, 90.0° Inc, 288.2°Az, 7316' SS and 3913' VS. A total of 1502 ft of produceable sand was drilled.

The purpose of this work is to evaluate a multilateral well drill onshore Niger Delta with D7.0 sand a target and design a procedure for accurate well placement and remain within the sweet spot (reservoir) using real-time resistivity, gamma and inclination data, thereby achieving optimal production of hydrocarbon from the reservoir.

METHODS OF STUDY

Drilling, trajectory, and petro-physical measurements were the three types of data used in geo-steering well 61. The largest source of data uncertainty that affected the wellbore location was the depth control. The best way that was used to deal with this depth problem was to investigate the quality of offset wells before starting the project (Sclumberger, 1995).

Problems with petro-physical data were also compared. Several different resistivity devices were used. They were compared to each other and to wire-line resistivity measurements. This was compounded by the effect of anisotropy at high angle and the degree of invasion at the time when this measurement was taken. Modelling helps to reduce this confusion. The magnitude of anisotropy was not known until after the formation was drilled. This caused significant error in the model. Before conducting the pre-drill geo-steering analysis, the true resistivity, dip angle and the lithology need to be determined (Burgess et. al., 1988). The true resistivity and dip angle need to be to determine from the actual resistivity tool response (Bittar et al., 2007; Bittar, 2002).

Estimates of the various lithologies are determined from the gamma ray log data, using Landers geo-steering software (Figure 1) and the flow chart for the extraction format is shown in Figure 2.

RESULTS AND DISCUSSION

Geosteering evaluation

Pre-well model was prepared using offset wire-line data from well 36, 51 and 58. Final models for both laterals were generated from the pilot hole MWD data (Table 1). Due to the high-hole inclination and formation dip the pilot hole data was converted to True stratigraphic thickness (TST) prior to modelling.

Lateral D7.0 build and land

The top D7.0 sand observed after sidetracking from the

Figure 1. Lander geosteering software.

pilot hole was at 7277 ft SS (8619 ftah), 2 ft TVD shallower than encountered in the pilot. As a result the landing depth was adjusted upwards by 2 ft to 7313 ft SS. The well followed the plan to the landing depth at 7314 ft SS, 1ft TVD below the intended position. The well landed in clean, homogeneous sands in the lower half of the D7.0 sand unit.

Lateral D7.0 – drain-hole

With the 7" liner shoe set at 8857 ftah drilling continued with the 4¾" MPR tool in the lateral section. The shallow 2 MHz phase resistivity was reading 100 to 240 Ω/m initially while the deeper reading 400 kHz attenuation resistivity read approximately 100 to 120 Ω/m (Table 2). Drilling continued along the planned well path at a high rate of penetration.

Resistivity response from both curves indicate that the entire drain hole length stayed well within the productive sand with no near shale response being apparent. It was decided to drill 1502 ft of drain hole that is slanted and terminating in the upper lobe of the shore face sand member. TVD window of 7315-7320 ft SS was given to the directional driller to ensure that the possibility of moving close to the POWC is minimized.

High gamma ray was observed throughout the drain without corresponding drop in resistivity values this was attributed to stringers of silty and/or radioactive sand in the drain. As drilling continued the hole angle was observed to be increasing and the TVD decreasing at the same time. Using the directional values transmitted with the model it became apparent that the well was approaching close to the roof. The directional driller could not slide to drop the angle because the mud motor was stalling and the tool face was very erratic. Due to the 4½" liner that was inadvertently dropped in hole an open-hole sidetrack was made and 1502 ft of drain was drilled with TD at 10359' MD. Resistivity gradually increased and levelled out to give about 100 Ω/m (Tables 3 and 4), for the 400 kHz AT and saturated 2 MHz PD of up to nearly 220 Ω/m. For the last 300' of hole the 400 kHz AT decrease from 100 to 56 Ω/m, indicating proximity to overlying shale (Figures 3 and 4).

The pre-well resistivity model based on the pilot hole correlated well with the MWD log from the landing point to TD. A polarization horn was seen as predicted at the top of the D7.0 sand due to the high resistivity contrast. The maximum resistivity value seen in the D7.0 sand was 2087 Ω/m. The deep reading 400 kHz attenuation resistivity was extremely useful as an indicator of structural position within the D7.0 sand. Its depth of investigation results in a curve that varies in value with depth as the distance between it and the overlying shale changes so that a correlation with the model can be used to indicate where the well is located in relation to the reservoir top (Prammer et al., 2007).

Model input data

Resistivity tool response data

Resistivity response (Figure 5) indicate that the entire

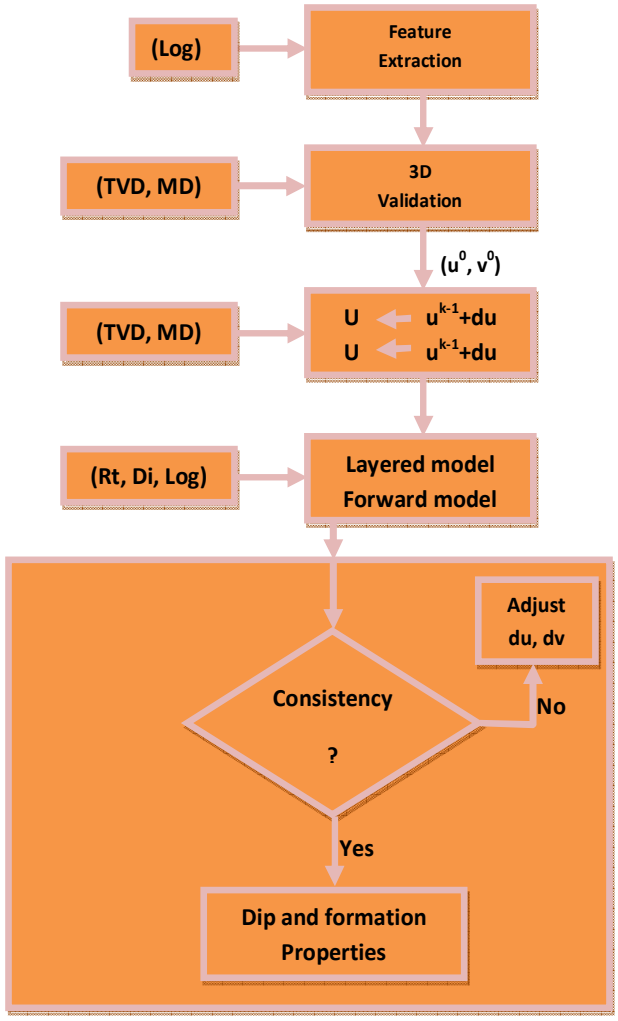

Figure 2. Flow chart for extraction format.

Table 1. Pilot hole / main hole formation tops.

Formation top	Pilot hole/main hole			Different	Prognosed tops	
D1.0	**MD**	**TVD**	**SS**	**+/-**	**TVD**	**SS**
D2.0	6610	6452	6344			
D3.0	6916	6643	6535			
D4.0	7283	6811	6703	-32	6843	6735
D5.0	7867	7032	6924			
D6.0	8230	7219	7111			
D7.0	8634	7387	7279	+29	7358	7250

drain hole length stayed well within the productive sand with no near shale response being apparent. It was decided to drill 1502 ft of drain hole and terminating in the D7. A TVD window of 7276-7282 (that is, ± 3 ft) instead of the ± 5 ft (Table 5) that was given to the directional driller to ensure that the possibility of removing close to the POWC is minimized. Low gamma ray was observed throughout the drain length without corresponding drop in resistivity values, thus was attributed to clean sand in the drain hole section.

The well landed 35 ft the top of D7 sand. It was evident from the correlation at landing that following the original

Table 2. Run summary data.

Run no.	Nine	Ten	Eleven	Twelve	Thirteen	Sixteen	Seventeen	Nineteen
Services type	**RNT**	**RNT**	**RNT**	**RNT**	**RNT**	**RNT**	**RNT**	**MPR**
Telemetry format	1 s Advantage combinatorial	1 s Advantage combinatorial	1 s Advantage combinatorial	1 s Advantage combinatorial	1 s Advantage combinatorial	1 s Advantage combinatorial	1 s Advantage combinatorial	1.5 s Advantage combinatorial
Resistivity transmitted	2 MHz PD 400 kHz PD 400 kHz AT	2 MHz PD 400 kHz PD 400 kHz AT	2 MHz PD 400 kHz PD 400 kHz AT	2 MHz PD 400 kHz PD 400 kHz AT	2 MHz PD 400 kHz PD 400 kHz AT	2 MHz PD 400 kHz PD 400 kHz AT	2 MHz PD 400 kHz PD 400 kHz AT	2 MHz PD 400 kHz AT
Tool size hole size	$8_{1/4}$" $12_{1/4}$"	$8_{1/4}$" $12_{1/4}$"	$8_{1/4}$" $12_{1/4}$"	$8_{1/4}$" $12_{1/4}$"	$8_{1/4}$" $12_{1/4}$"	$8_{1/4}$" $12_{1/4}$"	$8_{1/4}$" $12_{1/4}$"	$8_{1/4}$" 6"
Assembly type	Steerable 1.2 deg AKO	Steerable 1.2 deg AKO	Steerable 1.5 deg AKO	Steerable 1.4 deg AKO	Steerable 1.5 deg AKO	Steerable 2.4 deg AKO	Steerable 2.4 deg AKO	Steerable 1.3 deg AKO
Depth in	6458 ft	7064 ft	7185 ft	8383 ft	8992 ft	8281 ft	8427 ft	8772 ft
Depth out	7064 ft	7185 ft	8393 ft	8992 ft	9541 ft	8427 ft	8859 ft	8986 ft
Inclination range	42 - 61 degrees	62.4 degrees	58.1 - 72.9 degrees	66.6 – 78.1 degrees	78 – 80 degrees	59 – 61 degrees	66.05 – 86.39 Degrees	86.9 – 87.6 degrees
Mud type	SYNTEQ	SYNTEQ	SYNTEQ	SYNTEQ	SYNTEQ	SYNTEQ	SYNTEQ	SYNTEQ
Mud weight	0.52 - 0.54 psi/ft	0.54 psi/ft	0.54 psi/ft	0.54 psi/ft	0.54 psi/ft	0.54 psi/ft	0.54 psi/ft	0.54 psi/ft
RM @ temp	100 ohmm	100 ohmm	100 ohmm	100 ohmm	100 ohmm	100 ohmm	100 ohmm	100 ohmm
Reason for trip	BHA	BHA	BHA	MWD	TD PILOT Hole	BHA	Landing and casing point	NWD

Run no.	Twenty	Twenty one	Twenty two	Twenty three	Twenty four	Twenty five
Services type	**MPR**	**MPR**	**MPR**	**MPR**	**MPR**	**MPR**
Telemetry format	1.5 s Advantage combinatorial	1.5 s Advantage combinatorial	2.0 s Advantage combinatorial	2.0sec Advantage combinatorial	1.0 s Advantage combinatorial	1.0 s Advantage combinatorial
Resistivity transmitted	2 MHz PD 400 kHz AT	2 MHz PD 400 kHz AT	2 MHz PD 400 kHz AT	2 MHz PD 400 kHz AT	2 MHz PD 400 kHz AT	2 MHz PD 400 kHz AT
Tool size hole size	4 3/4" 6"	4 3/4" 6"	4 3/4" 6"	4 3/4" 6"	4 3/4" 6"	4 3/4" 6"
Assembly type	Steerable 1.3 deg AKO	Steerable 1.3 deg AKO	Steerable 1.6 deg AKO	Steerable 1.6 deg AKO	Steerable 1.8 deg AKO	Steerable 1.3 deg AKO
Depth in	8982 ft	9650 ft	8890 ft	9042 ft	7390 ft	7750 ft
Depth out	9650 ft	10162 ft	9042 ft	10359 ft	7750 ft	9440 ft
Inclination range	88 – 89.2°	89.7 – 91.85°	86.9 – 90.03°	86.9 – 87.6°	72.4 – 90.8°	85.2 – 90.9°
Mud type	SYNTEQ	SYNTEQ	SYNTEQ	SYNTEQ	SYNTEQ	SYNTEQ
Mud weight	0.54 psi/ft	0.54 psi/ft	0.50 psi/ft	0.50 psi/ft	0.48 psi/ft	0.48 psi/ft
RM @ temp	100 ohmm	100 ohmm	100 ohmm	100 ohmm	100 ohmm	100 ohmm
Reason for trip	BHA	TD	BHA	TD	BIT	TD

Table 3. Sensor offset to bit.

Run no.	Nine	Ten	Eleven	Twelve	Thirteen	Sixteen	Seventeen	Nineteen
Directional	59.91 ft	64.23 ft	59.82 ft	58.26 ft	58.58 ft	55.58 ft	60.00 ft	61.80 ft
Gamma ray	43.55 ft	47.87 ft	43.47 ft	41.98 ft	42.29 ft	43.54 ft	43.54 ft	37.27ft
Resistivity	44.82 ft	49.14 ft	44.74 ft	43.25 ft	43.56 ft	44.81 ft	44.81 ft	44.13 ft
Near bit inclination	42.59 ft	46.91 ft	42.51 ft	41.02 ft	41.33 ft	42.48 ft	42.58 ft	39.09 ft

Run no.	Twenty	Twenty one	Twenty two	Twenty three	Twenty five	Twenty six
Directional	61.80 ft	61.80 ft	60.80 ft	61.80 ft	61.80 ft	61.80 ft
Gamma ray	37.27 ft	37.27 ft	37.27 ft	37.27 ft	37.27 ft	37. 27 ft
Resistivity	44.13 ft	44.13 ft	44.13 ft	44.13 ft	44.13 ft	44.13 ft
Near bit inclination	39.07 ft	39.07 ft	39.07 ft	39.07 ft	39.07 ft	39.07 ft

Table 4. Final survey – lateral D7.0 sidetrack.

M.DPTH inclination Feet	CRS LEN Feet	Degrees	Azimuth Degrees	TVD Feet	Vert. sect. Feet	North/South Feet	East/West Feet	Dogleg sev. d/100’
0	0	0.00	0.00	0.00	0.00	0.00N	0.00E	TIEON
298	298	0.54	341.10	298.08	0.98	1.33N	0.45W	0.18
460	161	0.18	341.80	459.99	1.68	2.29N	0.78W	0.22
650	190	0.10	333.60	649.99	2.02	2.72N	0.96W	0.04
923	273	0.18	194.70	922.99	2.13	2.52N	1.17W	0.10
1295	371	0.74	235.82	1294.98	3.22	0.58N	3.29W	0.17
1483	188	0.68	222.80	1482.96	4.15	0.95S	5.03W	0.09
1767	284	1.00	218.10	1766.93	5.20	4.15S	7.69W	0.11
1859	92	1.20	232.85	1858.92	5.83	5.36S	8.95W	0.38
1954	95	0.74	217.12	1953.90	6.42	6.45S	10.11W	0.56
2047	92	0.65	212.99	2045.90	6.62	7.37S	10.76W	0.11
2142	95	0.17	165.77	2141.98	6.60	7.96S	11.02W	0.58
2334	192	0.19	154.13	2333.89	6.17	8.53S	10.81W	0.02
2621	287	0.53	219.59	2620.89	6.14	9.98S	11.45W	0.17
2984	283	0.40	337.40	2903.88	7.19	10.07S	12.66W	0.28
3102	198	0.90	97.02	3101.87	6.23	9.62S	11.35W	0.58
3196	94	1.13	82.71	3195.86	4.74	9.60S	9.73W	0.36
3250	94	2.23	74.34	3289.82	2.57	8.93S	7.05W	1.20
3385	95	3.87	65.75	3384.68	-0.91	7.17S	2.35W	1.79
3478	92	4.55	66.93	3477.43	-5.42	4.44S	3.91E	0.74
3574	96	3.89	70.66	3573.17	-10.28	1.87S	10.48E	0.74
3669	94	5.84	58.77	3667.82	-15.26	1.71W	17.66E	2.30
3764	95	6.95	61.57	3762.23	-21.36	6.95N	26.84E	1.21
3858	94	7.57	63.99	3855.48	-28.63	12.37N	37.41E	0.74
3953	94	9.33	62.95	3949.44	-37.28	18.62N	49.89E	1.86
4048	95	11.25	64.66	4042.91	-47.91	26.09N	65.13E	2.05
4141	92	9.80	67.98	4134.34	-59.07	32.94N	80.66E	1.69
4236	95	11.76	67.98	4227.66	-71.16	39.61N	97.13E	2.06
4302	66	11.76	67.90	4292.28	-80.29	44.67N	109.59E	TIEON
4380	78	10.13	65.00	4368.86	-102.27	50.56N	123.17E	
4477	97	6.73	52.68	4468.88	-111.84	57.61N	135.43E	3.95
4570	93	4.64	26.97	4557.36	-115.59	64.27N	141.47E	3.49
4660	98	4.6S	350.63	4647.09	-114.58	71.05N	142.54E	3.19

Table 4. Contd.

4764	104	3.92	325.95	4750.81	-109.92	78.07N	139.87E	1.84
4852	88	2.77	271.97	4838.68	-105.52	80.63N	136.06E	3.65
4947	95	3.85	266.50	4933.56	-100.95	80.55N	131.25E	0.41
5043	96	3.27	268.85	5029.41	-95.96	80.30N	125.96E	0.25
5139	96	3.86	289.84	5125.23	-90.17	81.26N	120.17E	1.48
5232	93	4.32	293.38	5217.99	-83.56	83.67N	114.00E	0.60
5325	93	5.45	294.23	5310.69	-75.69	86.87N	106.75E	1.22
5423	5423	8.39	299.81	5483.64	395.01	197.03N	343.9SW	0.15
5520	97	11.13	302.33	5499.23	411.35	205.55N	357.9SW	2.86
5615	95	12.15	301.71	5592.27	430.38	215.72N	374.21W	1.03
5710	95	13.49	304.14	5684.92	451.25	227.19N	391.88W	1.52
5885	95	15.38	307.39	5776.90	474.51	241.06N	411.07W	2.16
5981	96	21.34	309.65	5867.83	524.26	268.21N	434.9W	6.77
5996	95	26.17	309.34	5954.68	541.69	284.78N	464.78W	4.56
6091	95	29.47	307.22	6038.61	584.86	312.20N	499.6W	3.63
6184	93	32.12	303.25	6118.50	631.71	338.60N	538.5W	3.59
6278	94	34.84	300.37	6196.92	683.20	305.88N	582.58W	3.35
6374	96	38.17	299.61	6274.05	740.00	395.41N	632.04W	3.50
6470	96	41.93	298.88	6347.53	881.69	425.56N	685.94W	3.95
6567	97	44.99	298.50	6417.93	868.27	457.57N	744.47W	3.16
6662	95	47.77	297.94	6483.46	936.94	498.08N	805.07W	2.96
6757	95	50.95	297.71	6545.32	1008.94	523.72N	868.82W	3.35
6848	91	54.30	298.05	6600.24	1081.39	557.65N	932.94W	4.24
6944	95	58.02	295.69	6653.34	1161.22	595.65N	1003.29W	3.40
7033	89	61.00	298.71	6692.49	1237.75	632.48N	1070.55W	3.35
7155	82	62.40	299.26	6737.37	1309.78	687.46N	113.78W	1.81
7235	119	66.62	300.30	6789.08	1417.71	721.27N	1227.65W	3.52
7340	105	71.92	301.13	6826.15	1515.41	771.42N	1312.07W	5.10
7435	96	72.98	300.72	6855.17	1888.45	818.44N	1990.58W	1.10
3531	94	70.64	301.11	6884.96	1695.18	884.78N	1467.96W	2.51
7625	94	67.16	299.71	6918.87	1783.46	909.16N	1543.55W	3.58
7720	94	63.70	296.22	6958.38	1869.71	949.69N	1619.81W	4.94
7816	96	61.46	289.52	7002.63	1954.79	982.83N	1698.24W	6.62
7909	92	60.15	288.39	7047.99	2035.51	1000.21N	1775.02W	1.76
8006	97	58.83	286.47	7097.24	2118.32	1834.24N	1856.74W	2.18
8101	95	59.11	285.27	7145.21	2198.67	1850.50N	1933.04W	1.12
8195	94	58.14	287.30	7195.15	2277.97	1079.00N	2010.07W	2.11
8286	91	59.47	287.37	7245.57	1912.05	997.51N	1644.17W	TIEON
8358	72	61.07	286.84	7282.27	1930.55	1815.90N	1703.93W	2.31
8453	95	66.05	283.83	7324.57	2015.51	1838.34N	1785.93W	5.96
8553	100	68.75	278.76	7363.01	2187.24	1856.37N	1876.43W	5.41
8648	95	73.87	281.64	7393.44	2183.47	1872.33N	1984.60W	6.10
8707	89	81.39	283.32	7412.49	2283.80	1891.12N	2249.77W	8.65
8795	58	86.39	284.65	7418.66	2340.55	1105.06N	2105.71W	8.92
8863	68	87.56	287.06	7422.25	2408.42	1123.61N	2171.02W	3.94
8286	8286	59.47	287.37	7246.57	1912.05	997.51	1644	TIEON
8358	72	61.07	286.84	7282.27	1930.55	1815.90	1703.90	2.31
8453	95	66.05	283.83	7324.57	2015.51	1838.34	1785.93	5.96
8553	100	68.05	278.76	7363.01	2487.24	1856.37	1876.43	5.41
8648	95	73.87	281.64	7393.44	2196.47	1872.33	1964.9	6.10
8737	89	81.39	283.362	7412.49	2283.00	1891.12	2846.77	8.65
8795	58	8639	284.65	7418.66	2340.55	1105.06	2105.71	8.92

Table 4. Contd.

8863	68	87.56	287.86	7422.25	2488.42	1123.61	2171.02	3.94
8890	27	87.71	266.79	7423.36	2435.40	1181.40	3196.8	TIEON
8947	57	86.85	284.23	7428.07	2501.91	1146.62	2251.72	4.73
020	73	91.79	284.65	7426.93	2574.66	1184.82	2322.38	6.79
9113	93	91.70	286.72	7424.10	2667.46	1189.95	2411.87	2.23
9207	94	89.63	288.96	7423.01	2761.43	1218.74	2501.34	3.24
9328	121	88.98	289.92	7424.48	2882.41	1259.07	2615.43	0.96
9397	69	89.20	288.81	7425.57	2951.40	1257.89	2680.52	1.64
9524	127	88.98	286.36	7427.59	3078.34	1320.25	2801.56	1.94
9620	96	91.23	285.43	7427.41	3174.20	1346.54	2893.88	2.54
9683	63	91.66	285.39	7425.82	3237.06	1833.27	2954.55	0.63
9778	95	89.14	285.80	7425.16	3331.89	1355.81	3246.05	2.69
9873	95	90.12	285.93	7425.77	3426.75	1414.78	3137.47	1.04
9968	95	90.62	286.37	7425.16	3521.64	1441.20	3228.71	0.70
10063	95	0.89	287.85	7423.91	3616.58	1480.16	3319.58	1.50
10159	95	89.17	288.17	7423.66	3712.56	1498.85	3410.75	1.82
10254	95	89.85	288.21	7424.67	3887.55	1528.50	3501.04	0.72
10360	106	90.80	288.20	7424.81	3913.54	1581.62	3601.73	0.14

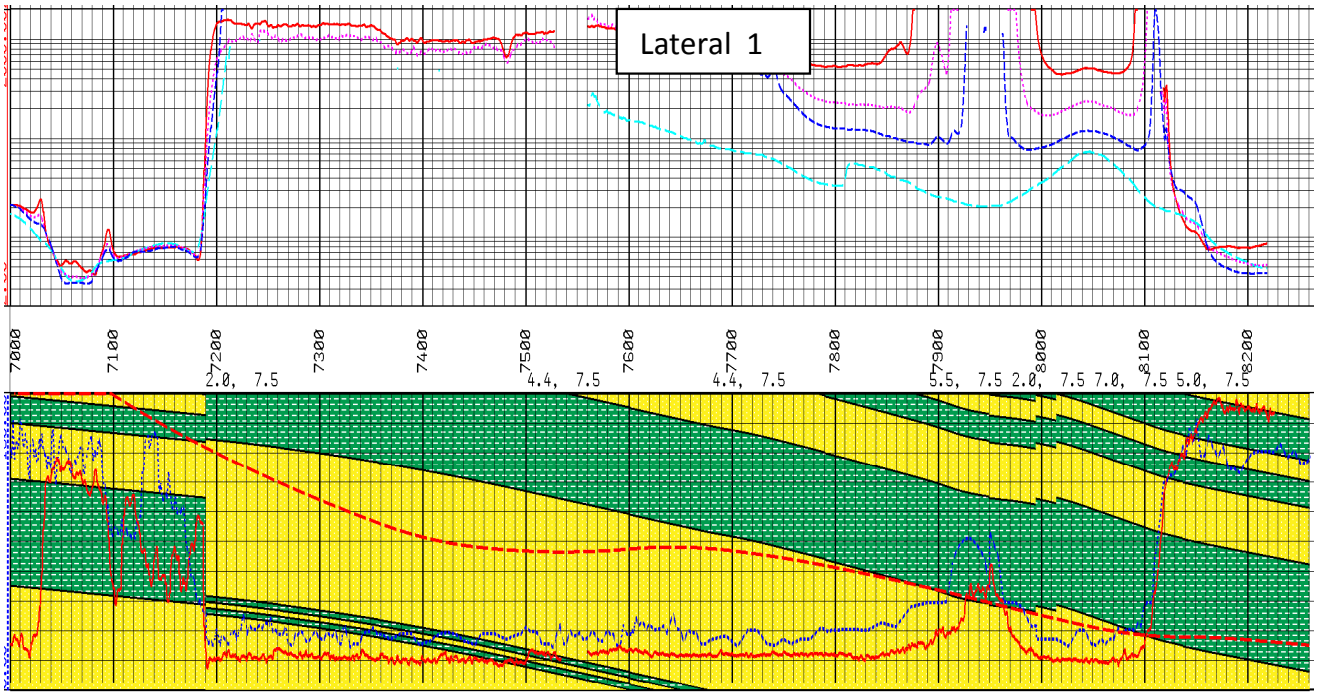

Figure 3. Geosteered well to optimize wellbore placement.

well plan would place the well inside the water zone (Figure 6). Therefore the drilling plan was modified, where a tangent section was drilled to land the well at the top of D7 prior to geo-steering to a further improved, net to gross ratio. Require that the driller steer up 89.9° and to the right (azimuth) at the beginning of reach section, continue like that to 90° (Table 6) until the well reach total depth.

The proposed well plan was based on the earth model, with torque and drag computation used to verify that

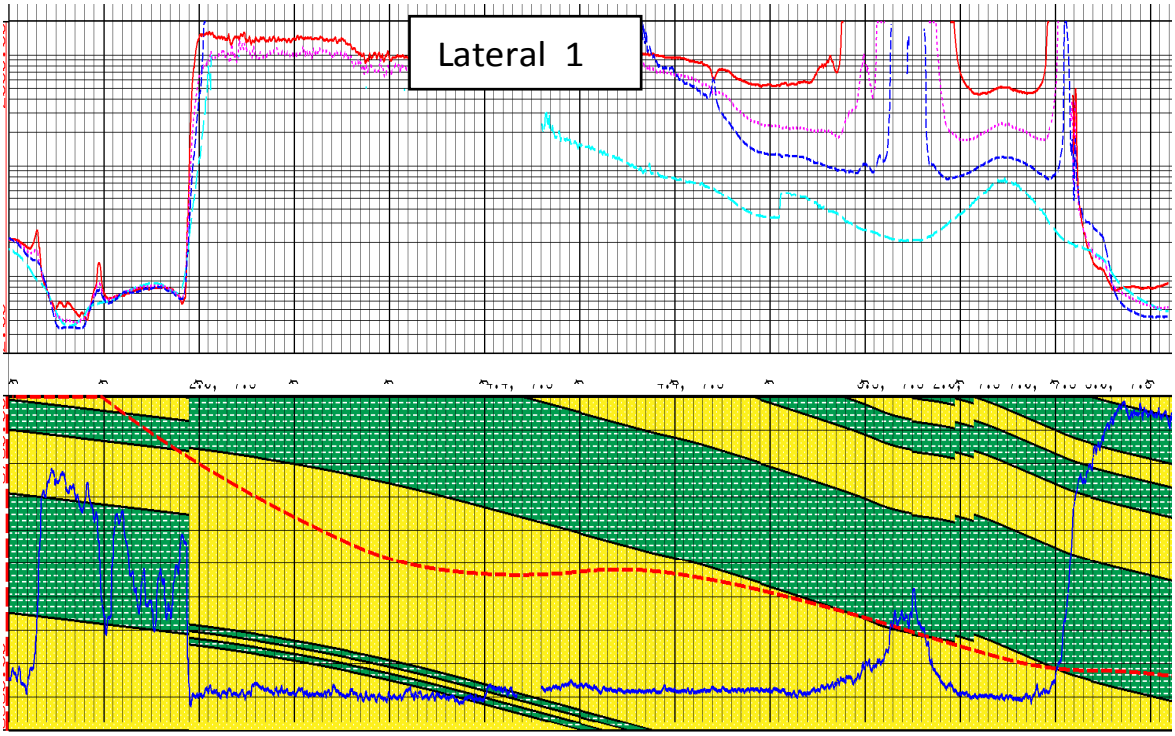

Figure 4. Geosteered well to optimize wellbore placement.

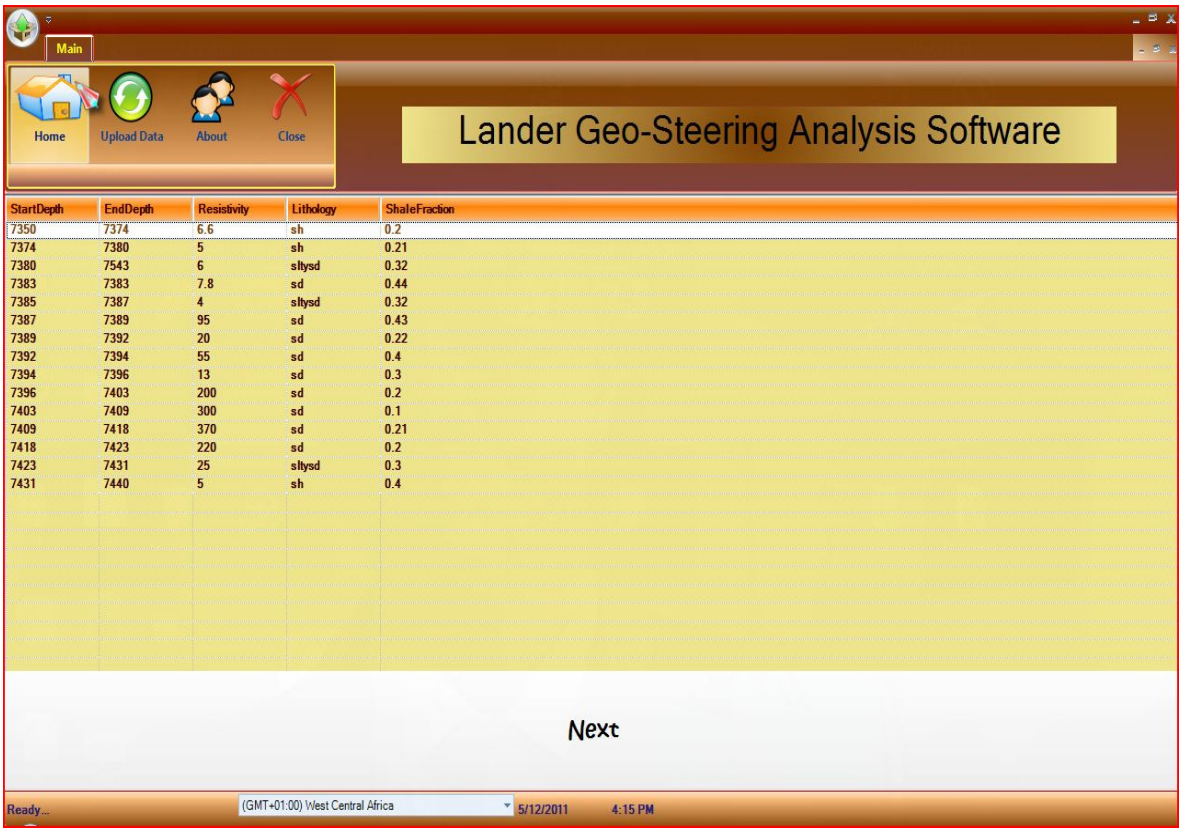

Figure 5. Offset well resistivity tool response data.

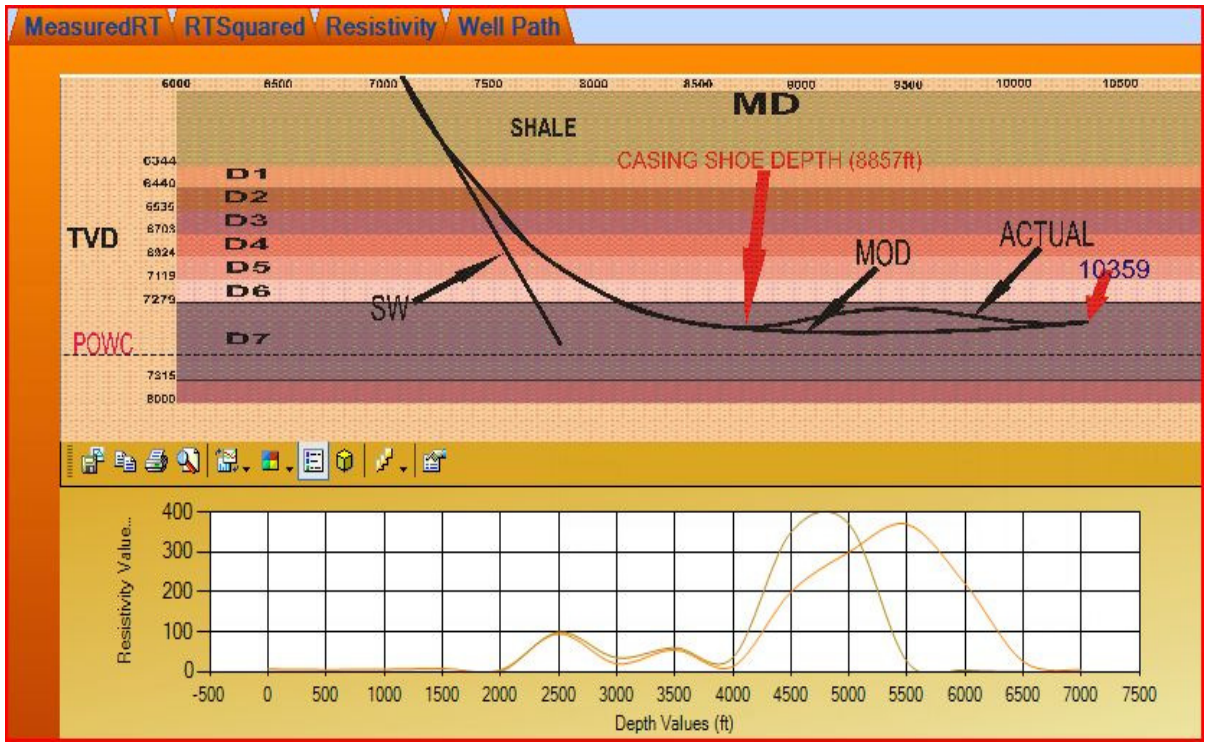

Figure 6. Proposed, actual and initial offset modeled well path.

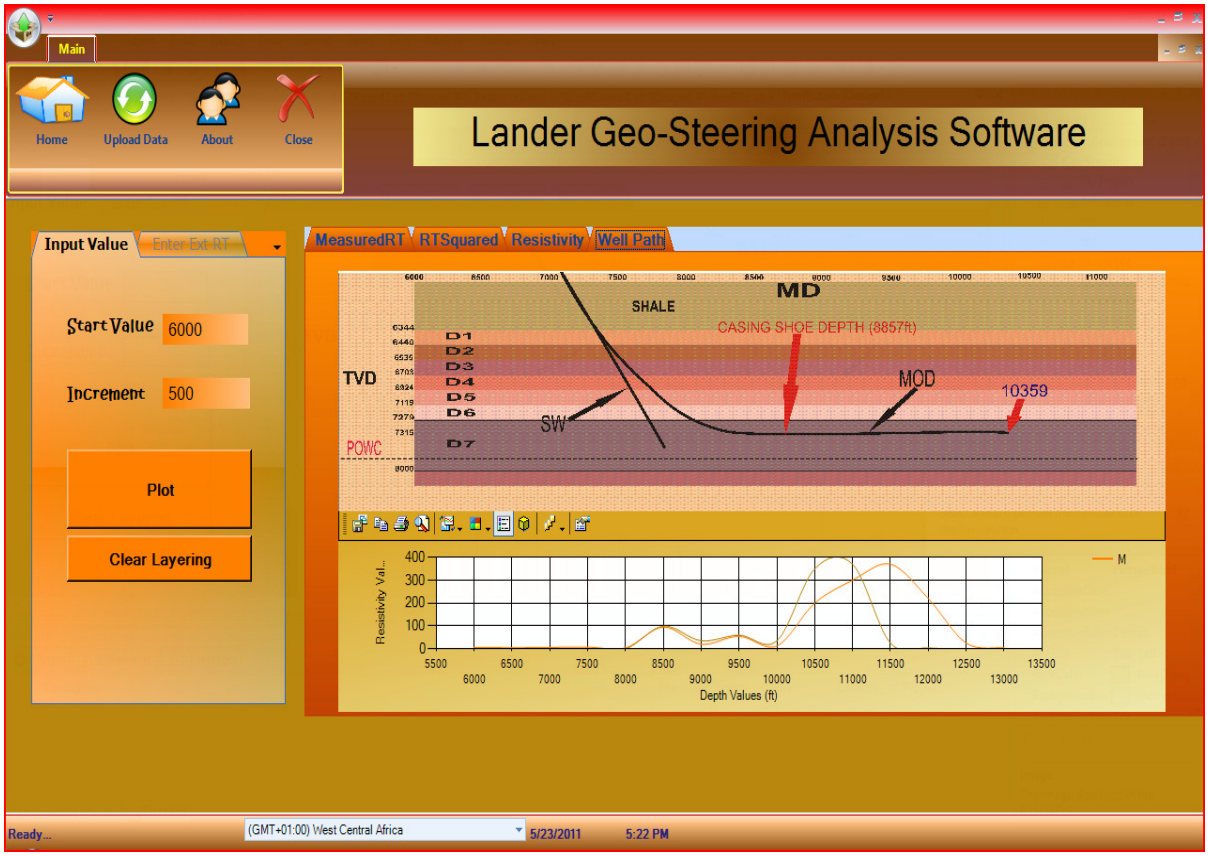

Figure 7. Proposed and offset well path.

Table 5. Final resistivity profile – lateral D7.0.

Profile based on well 61 pilot hole MWD Log			
Start depth Ftss	**End depth fitness**	**RTohm m**	**Lithology**
7350	7374	6.6	sh
7374	7380	5	sh
7380	7383	6	slty sd
7383	7385	7.8	sd
7385	7387	4	sltst
7387	7389	95	sd
7389	7392	20	sd
7392	7394	55	sd
7394	7396	13	sd
7396	7403	200	Sd
7403	7409	300	Sd
7409	7418	370	Sd
7418	7423	220	Sd
7423	7431	25	Slty sd
7431	7400	5	Sh

Table 6. Final formation dip breakdown.

These estimated bed dips for the D7.0 sand unit were derived real-time from the geosteering model. Measured depth (ftah)	Formation dip (degree)	Dip Azimuth (degrees)	Reservoir top (ft TVD)	Reservoir top (ftss)
8500	4.5	275.0	7376.4	7268.4
8550	4.5	275.0	7380.1	7272.1
8600	4.5	275.0	7383.8	7275.8
8650	4.3	264.0	7387.4	7279.4
8700	4.1	249.1	7390.6	7282.6
8750	3.9	235.6	7393.2	7285.2
8800	3.8	232.7	7395.3	7287.3
8850	3.8	229.8	7397.3	7289.3
8900	3.7	227.0	7399.0	7291.0
8950	3.6	224.1	7400.6	7292.6
9000	3.6	221.2	7402.1	7294.1
9050	3.5	218.3	7403.4	7295.4
9100	3.4	215.4	7404.4	7296.4
9150	3.4	212.5	7405.3	7297.3
9200	3.3	210.0	7405.9	7297.9
9250	3.3	210.0	7406.5	7298.5
9300	3.3	210.0	7407.0	7299.0
9350	3.3	210.0	7408.1	7300.1
9400	3.3	210.0	7408.7	7300.7
9450	3.3	210.0	7409.3	7301.3
9500	3.3	210.0	7410.0	7302.0
9550	3.3	208.3	7410.2	7302.2
9600	3.3	195.0	7410.2	7302.2
9650	3.3	195.0	7410.2	7302.2
9700	3.3	195.0	7410.1	7302.1
9750	3.3	195.0	7410.1	7302.1
9800	3.3	195.0	7410.1	7302.1

Table 6. Contd.

9850	3.3	195.0	7410.0	7302.1
9900	3.3	195.0	7410.0	7302.0
9950	3.3	195.6	7410.0	7302.0
10000	3.3	201.2	7410.0	7302.0
10050	3.3	210.0	7410.5	7302.5
10100	3.3	210.0	7411.1	7303.1
10150	3.3	210.0	7411.7	7303.7
10200	3.3	210.0	7412.3	7304.3
10250	3.3	210.0	7412.9	7304.9
10300	3.3	210.0	7413.4	7305.4
10350	3.3	210.0	7414.0	7306.0
10359	3.3	210.0	7414.2	7306.2

Lateral D7.0 ; • 1:1000 MD correlation RWD/model log –landing and drain.

drilling the proposed well plan was possible (Figure 7).

Conclusion

The use of slant well path would have landed the well path out of the D 7 sand, because it is shaling out (High gamma ray and low resistivity values down D 7). Using the initial modeled well path of the offset well, would have landed the well 1 ft away from the water zone. But after careful review and analysis of the offset well geosteering data, it was observed that landing the well 10.5 ft (3.15 m) away from the top of D 7 or from the pseudo fluid contact will place the well optimally within the reservoir.

The increasing confidence with which horizontal wells are being drilled is leading the way to targeting smaller volumes of the reservoir. While 3D seismic and offset data are able to constrain geological uncertainty when drilling these targets, there is an increasing need to fine tune the trajectory to improve the well position and so maximize hydrocarbon productivity and recovery.

Proper Geosteering helps to maximize the reservoir contact in many types of reservoirs, resulting in optimal initial production rates. Deep resistivity sensor measurements enable Geosteering based on the resistivity contrast between the reservoir and the overlying and underlying intervals.

The pre-well resistivity model correlated well with the offset well log from the landing point to the TD. Therefore this model can be used to drill any prospective well in the same oil field. Lander Software integrates the information and inverts it in real time for placing the well within the geological layers, and for updating the geology.

The techniques and examples provided in this project give an overview of what has been achieved to date. For the future, the very cost effectiveness of the Geosteering process will guarantee its continued use in many of the horizontal wells still waiting to be drilled.

REFERENCES

Al-Mutari B, Jumah S, Al-Ajmi H, Saleh KM, Burman JR, Reeves D (2009). “Geosteering for Maximum Contact in Thin-Layer Well Placement”, SPE-120551, presented at the SPE Middle East Oil and Gas Show and Conference, Kingdom of Bahrain.

Bittar M (2002). “Electromagnetic Wave Resistivity Tool Having A Tilted Antenna For Geosteering Within A Desired Payzone”, US Patent 6:476-609.

Bittar M, Klein J, Beste R, Hu G, Wu M, Pitcher J, Golla C, Althoff G, Sitka M, Minosyam V, Paulk M (2007). “A New Azimuthal Deep-Reading Resistivity Tool for Geosteering and Advanced Formation Evaluation”, SPE-109971, presented at the SPE Annual Technical Conference and Exhibition, Anaheim.

Burgess T, Falconer IG, Sheppard M (1988). “Separating Bit and Lithology Effects from Drilling Mechanics Data”, SPE/IADC-17191.

Omeragic D, Li Q, Chou L, Yang L, Duong K, Smits J, Lau T, Liu CB, Dworak R, Dreuillault V, Yang J, Ye H (2005). "Deep Directional Electromagnetic Measurements for Optimal Well Placement," SPE-97045, presented at the SPE Annual Technical Conference and Exhibition, Dallas, Texas.

Peach SR, Kloss PJC (1994). “A New Generation of Instrumented Steerable Motors Improves Geosteering in the North Sea.”, SPE/IADC-27482.

Prammer MG, Morys M, Knizhnik S, Conrad CJ, Hendricks WE, Bittar MS, Hu G, Hveding F, Kenny K, Shokeir RM, Seifert DJ, Neuman PM, Al-Dossari S (2007). “Field Testing of an Advanced LWD Imaging/Resistivity Tool”, presented at the SPWLA 48th Annual Logging Symposium.

Sclumberger (1995). “Fundamentals of Horizontal Well Planning, Geosteering And Formation Evaluation.” Schlumberger Documentation.